Clay Minerals (2003) **38**, 141–150

Evaluation of talc morphology using FTIR and H/D substitution

E. FERRAGE[1,*], F. MARTIN[2], S. PETIT[3], S. PEJO-SOUCAILLE[4], P. MICOUD[5], G. FOURTY[4], J. FERRET[4], S. SALVI[5], P. DE PARSEVAL[5] AND J. P. FORTUNE[5]

[1] *Groupe Géochimie de l'Environnement, LGIT, Maison des Géosciences, Université Joseph Fourier, CNRS, BP 53, 38041 Grenoble cedex 9, France,* [2] *LASEH, UMR 6532 HYDR'ASA, Université de Limoges, 123 Avenue Albert Thomas, Bât. Les Dryades, 87000 Limoges, France,* [3] *Laboratoire Hydr'ASA, Université de Poitiers-CNRS, 40, avenue du Recteur Pineau, F-86022 Poitiers Cedex, France,* [4] *Talc de Luzenac S. A., BP 1162, F-31036 Toulouse Cedex, France, and* [5] *Equipe Géomarg, LMTG, 39, allées Jules Guesde, Université Paul Sabatier-CNRS, 31000 Toulouse, France*

(*Received 5 October 2000; revised 9 July 2002*)

ABSTRACT: Deuteration (H/D substitution at 200ºC) was performed on powders of two ground talcs of different particle shapes (different basal/lateral surface ratios). Results indicate that the deuteration process is only efficient on lateral talc surfaces, and suggest that the hydrogens located in the hexagonal ring of the talc basal surfaces are not exchanged. The FTIR spectra collected from the two talc samples show that it is possible to discriminate between particles with the same specific surface area but with different basal/lateral surface ratios using the deuteration process.

KEYWORDS: talc, particle morphology, FTIR, deuteration.

Talc is used as filler in many industrial applications such as paper, paint, ceramics and polymers (Menczel & Varga, 1983; Ferrage *et al.*, 2002). Material modifications (functionality) induced by talc are due to chemical inertness, the particle aspect ratio (lamellarity) and hydrophobic properties of this mineral. In polymer applications, even a small increase in the amount of talc stabilizes and stiffens automobile parts such as fenders, dashboards or steering wheels. To assess the potential of the different talc products, their lamellarity needs to be characterized. Different talc morphologies are observed ranging from long and well-stacked up flakes (so-called 'macrocrystalline' type) to an heterogeneous stack of small plates ('microcrystalline' type). These two terms are also used in an industrial sense to describe particle shapes, 'macrocrystalline' and 'microcrystalline' products having high and low basal/lateral surface ratios, respectively. This aspect ratio is strongly dependent on the formation conditions of the talc deposits (Fortuné *et al.*, 1980; Moine *et al.*, 1989; de Parseval *et al.*, 1993).

To transform the ore rock into a fine powder, wet or dry milling procedures are used even though wet milling can induce a cementation of fine particles for some products. In polymer applications, talc products showing a high basal/lateral surface ratio with a high specific surface area (SSA) and having a low degree of cementation are preferred. However, it is difficult to predict particle morphology, especially for small particle sizes, if talcs from two different deposits have the same SSA. Nevertheless, the morphology (e.g. basal/lateral surface ratios) of the talc particles is the main physical parameter that determines whether a specific talc is suitable for a specific application or not.

* E-mail: Eric.Ferrage@obs.ujf-grenoble.fr
DOI: 10.1180/0009855033820084

Use of D_2O in hydrothermal synthesis is a common method for identifying the infrared (IR) absorption bands (Stubican & Roy, 1961; Farmer *et al.*, 1968; Russel *et al.*, 1970; Shirozu & Ishida, 1982; Ishida, 1990; Grauby *et al.*, 1991; Martin *et al.*, 1999), because of the conversion of some, or all, of the OH groups to OD groups. When D replaces H in talc, the difference in atomic mass induces a shift of the OH vibration, in the Fourier Transform infrared (FTIR) spectrum, towards lower wavenumbers characterized by a factor R defined as:

$$R = \frac{\nu Mg_3OH}{\nu Mg_3OD}$$

Thus, as R is close to 1.37 for a pure librational frequency (Langer & Lattard, 1980), it allows the degree of H-D exchange to be easily determined using IR spectroscopy.

In this study, the degree of exchange was measured for two types of talc having differently shaped particles, each exhibiting a range of specific surface areas. The aim was, first, to determine the location of the H-D substitution in the talc structure and, secondly, to discriminate between particle shapes using FTIR and deuterated samples.

TABLE 1. BET specific surface areas obtained for talcs A and B after different milling times.

	Specific surface area* (m^2/g)					
Talc A	7	11.5	17.5	30.5	47.5	60
Talc B	7.5	13	21	27		

* ± 1 m^2/g

MATERIALS AND METHODS

We used a pure talc sample composed of very well defined cm-sized plates from Brazil (M – mineralogical collection, Toulouse, France) as a refer-

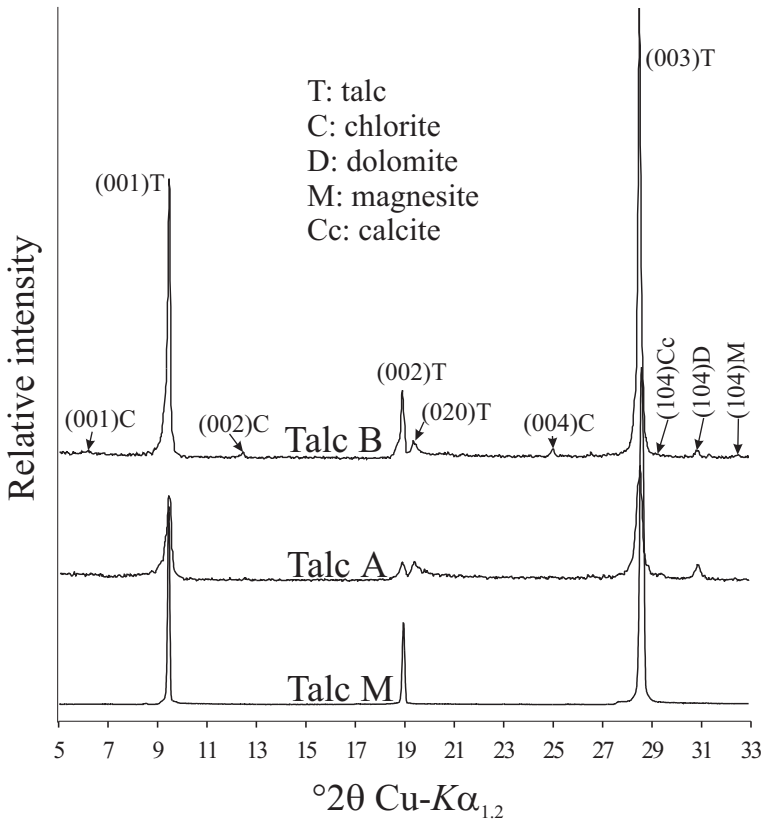

FIG. 1. XRD patterns of talcs A, B and M.

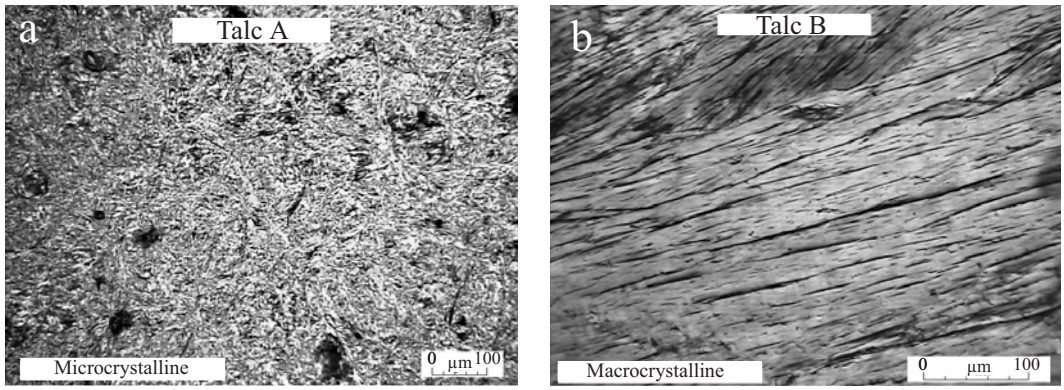

FIG. 2. Optical micrographs of talcs A (a) and B (b) morphologies.

ence. Two additional talc samples, A and B, were described as 'microcrystalline' and 'macrocrystalline' specimens, respectively. These two talc varieties were commercial products obtained from S.A. Talc de Luzenac (Toulouse, France).

Talc samples A and B were ground in an Alpine® grinder, using various grinding times depending on the propensity for particle breaking of the talc. The resulting powders exhibit a wide range of BET specific surface areas (BETSSA, Table 1). The BETSSA were measured with a Micromeritics FlowSorb II 2300 under an Ar flow. Particles with specific surface areas of ~7 $m^2\ g^{-1}$ correspond to those normally used for commercial purposes. The difference in the BETSSA maximum value for the two specimens is due to the fact that microcrystalline talc is more easily ground than the macrocrystalline variety.

TABLE 2. Chemical compositions (wt.%) of talcs A and B, obtained by XRF spectroscopy.

Oxides	Talc A	Talc B
SiO_2	57.58	59.56
Al_2O_3	0.44	0.82
Fe_2O_3	0.37	0.74
MgO	29.82	30.48
CaO	1.82	0.58
K_2O	0.002	0.015
Na_2O	0.003	0.012
TiO_2	<0.1	<0.1
L.O.I.*	8.41	6.63
Total	98.45	98.84

* L.O.I.: Loss on ignition at 1050ºC

The chemical compositions of talc samples A and B were determined by X-ray fluorescence (XRF) using a Philips PW 2404 X-ray spectrometer equipped with a rhodium anode (4 kW). The composition of talc M was determined using a Cameca SX50 electron microprobe. The operating conditions were 15 kV and 10 nA using natural and synthetic standards for calibration. X-ray diffraction (XRD) patterns were obtained on a Philips X'Pert, using reflection mode on randomly oriented powders with Ni-filtered Cu-$K\alpha$ radiation (40 kV, 55 mA). Talc morphologies were observed by optical microscope under crossed polarizers. The effects of milling on the talc powders were observed using a LEO 435 VP scanning electron microscope (SEM).

All the products were subsequently reacted with D_2O (100.0 atomic %D, Acros Organics, New Jersey, USA) at 200ºC, in teflon-coated metal

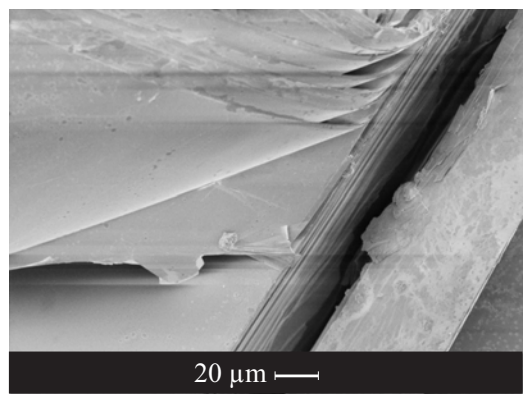

FIG. 3. Extended sheets in (*a,b*) plane of talc M by SEM.

bombs for 5 days. The FTIR spectra were recorded in the 4000−400 cm^{-1} range using a Nicolet 510 spectrometer. Pellets were prepared by mixing a 1.2 mg sample with 200 mg of KBr. Spectra were normalized in intensities with respect to the Si−O-vibration band at 1018 cm^{-1}. Diffuse reflectance infrared (DRIFT) spectra were recorded using the DRIFT accessory 'Collector' from Spectra-Tech.

Complexation experiments were performed by placing a 1 g aliquot of talc with 0.2 g of EDTA salt (disodium ethylenediaminetetracetic acid) in 1 dm^3 of bi-distilled water at 25ºC for 5 days to complex free cations in solution. The samples were then dried and reacted with D_2O at 200ºC for 5 days.

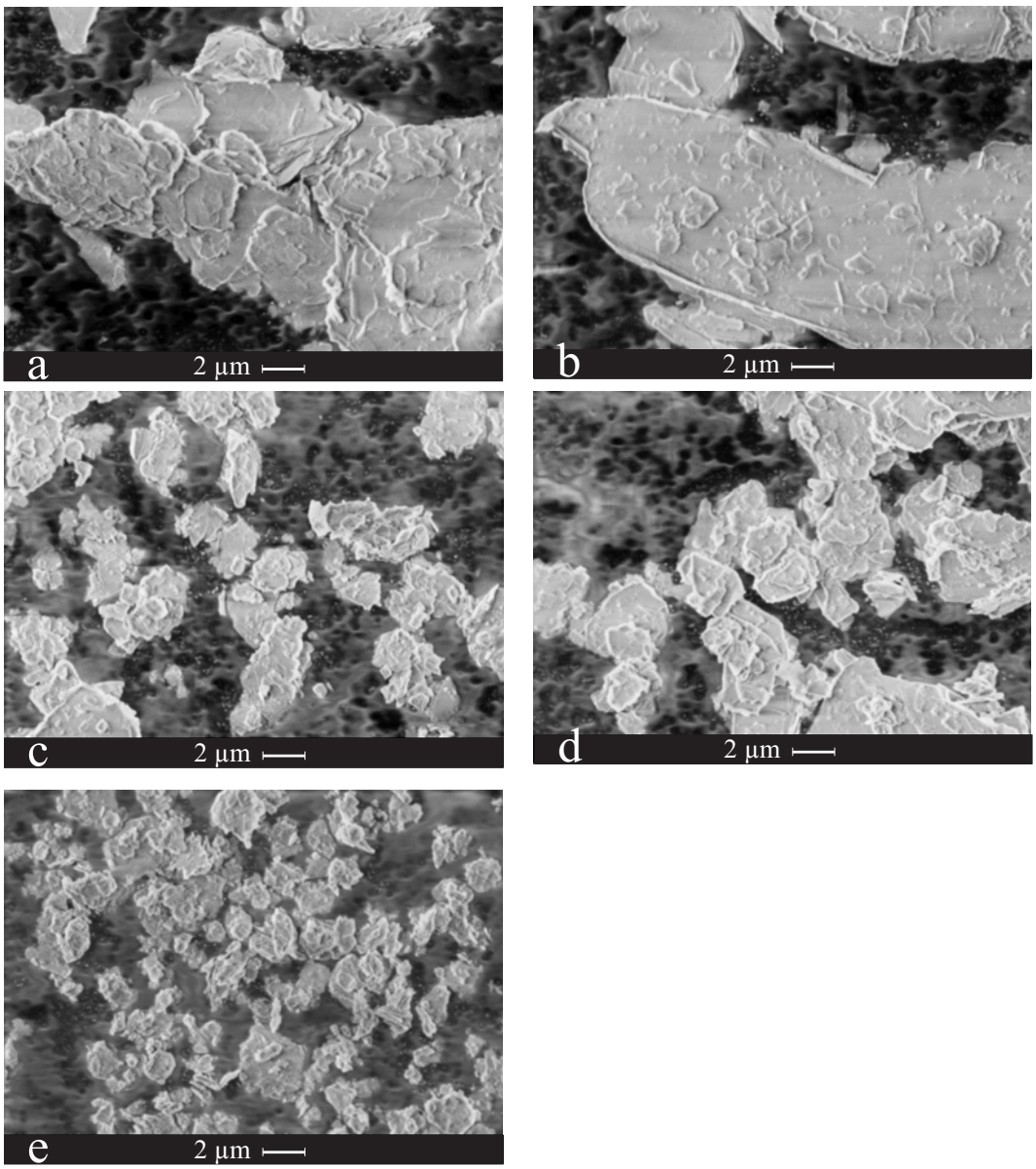

FIG. 4. Particle forms of talcs A and B with various BETSSA values: 7 (a), 47.5 (c) and 60 $m^2\ g^{-1}$ (e) for talc A; 7.5 (b) and 27 $m^2\ g^{-1}$ (d) for talc B by SEM.

RESULTS AND DISCUSSION

Talc composition

The XRD pattern of sample A reveals the presence of small amounts of dolomite (<2%) and of calcite traces in addition to talc (Fig. 1). Sample B contains traces of chlorite, dolomite, calcite and magnesite (<2%). No impurity is detected in talc sample M (Fig. 1).

Chemical analyses of samples A and B reveal the presence of minor amounts of CaO, consistent with the presence of carbonates (Table 2). The chemical formula of talc M, calculated from electron microprobe analysis, is $(Fe_{0.14}Mg_{5.86})[Si_8O_{20}(OH)_4]$.

Talc morphology

Figure 2a shows very small aggregated flakes (<50 μm) of untreated talc A with no specific arrangement, in agreement with the microcrystalline character of this talc. In sample B, untreated talc flakes occur as well-stacked mm-sized sheets

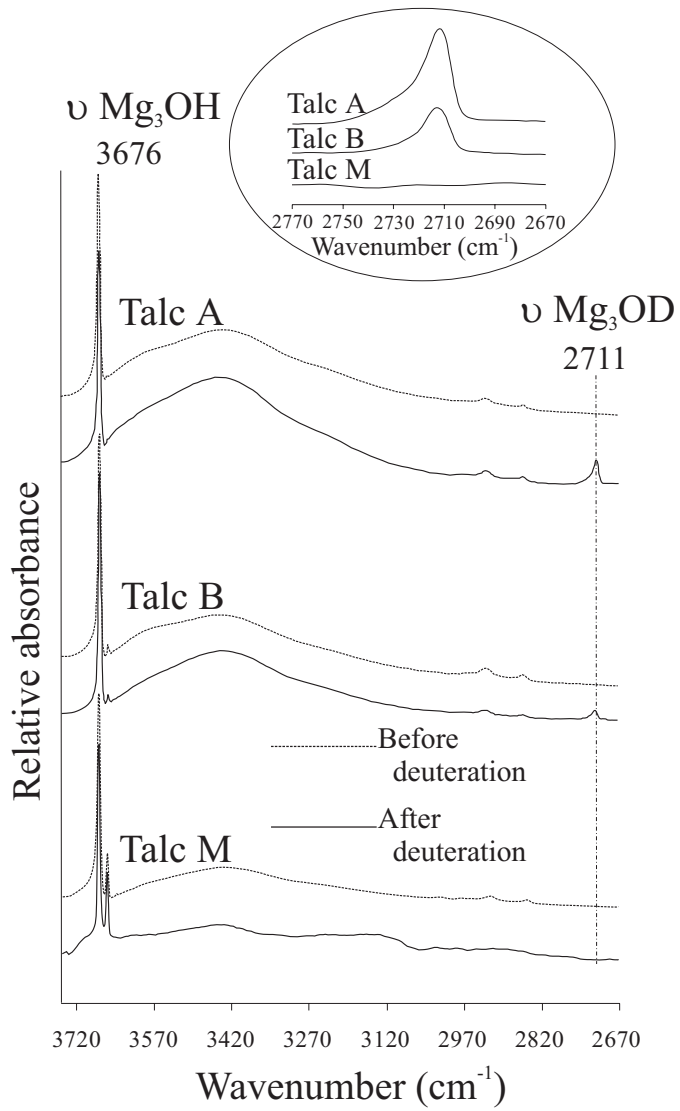

FIG. 5. FTIR spectra of talcs A (60 $m^2\ g^{-1}$), B (27 $m^2\ g^{-1}$) and M, before and after deuteration in the OH-OD region (3750–2650 cm^{-1}). Talc M after deuteration was recorded by DRIFT spectroscopy.

(Fig. 2b) reflecting the macrocrystalline character of this sample.

Figure 3 shows the smooth sheets of talc M extended in the (*a,b*) plane as seen by SEM. One may note on Fig. 3 that a few sheets were turned upside-down during sample preparation. After milling, leading to similar specific surface areas for the two samples (7 $m^2 g^{-1}$), sample A clearly shows a heterogeneous arrangement of small flakes (low basal/lateral surfaces ratio – Fig. 4a), whereas sample B is composed of particles with higher basal/lateral surface ratios (Fig. 4b). During milling, specific surface areas increase and particle size decreases. Even if the milling process clearly increases the fragmentation of talc particles (Fig. 4c–e), it is difficult to know if the contrasting particle morphologies observed previously (Figs 2a,b) are retained during this process.

FTIR

The FTIR data collected after deuteration of talc A (BETSSA 60 $m^2 g^{-1}$) and talc B (BETSSA 27 $m^2 g^{-1}$) show the Mg_3OD vibrational band at 2711 cm^{-1} (Fig. 5), giving an *R* factor of 1.356. To discriminate between H/D substitutions onto particle edges and onto basal surfaces, FTIR data were collected on the basal planes of talc M after deuteration, using the reflection mode (DRIFT) on a few μm^2 of surface (Fig. 5). The presence in all spectra of a band located at 3660 cm^{-1} is related to a $(Mg_2,Fe)OH$ vibration mode (Wilkins & Ito, 1967). No band corresponding to the Mg_3OD vibration could be observed on the FTIR spectrum recorded on the surface of talc M (Fig. 5), indicating that there is no H-D substitution on the basal surfaces of talc under these experimental

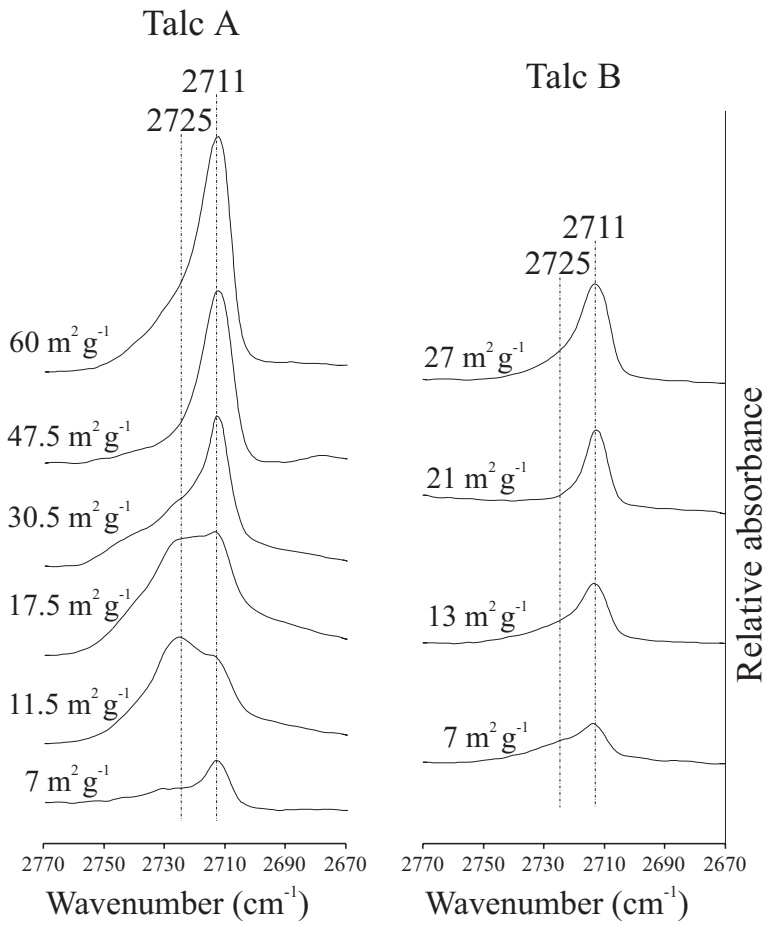

FIG. 6. FTIR spectra of talcs A and B with various specific surface areas in the OD region (2770–2670 cm^{-1}).

conditions and that exchange occurs only on the lateral surfaces. According to DRIFT results, hydrogen atoms located in the hexagonal ring are not exchanged at 200ºC after reaction with D_2O. On the other hand, the intensity of the Mg_3OD band (2711 cm^{-1}) increases with increasing BETSSA for both talc samples (Fig. 6). In addition, a large band is observed near 2725 cm^{-1} for all ground samples of talc A. This band is also present in spectra recorded on talc B samples but shows a lower intensity.

Attribution of the 2725 cm^{-1} absorption band

After deuteration of sample A, the band at 879 cm^{-1}, related to the presence of dolomite, disappeared whereas a vibration band relative to calcite appeared (Fig. 7). This observation is in agreement with XRD data (Fig. 8) showing that the (104) reflection of dolomite is no longer visible after deuteration whereas the intensity of the calcite (104) reflection clearly increased after this treatment (Fig. 8). In addition, in the 1700–1300 cm^{-1} region, the νCO_3 band is less intense after deuteration than it was before (Fig. 7).

After complexation of talc A with EDTA, vibrational bands related to carbonates are no longer observed in the 910–850 cm^{-1} and 1700–1300 cm^{-1} regions in the FTIR spectra (Fig. 7), suggesting that EDTA treatment removed all the carbonates. In addition, after complexation with EDTA and deuteration treatment, two ground samples of talc A (11.5 and 60 $m^2\ g^{-1}$) do not exhibit the 2725 cm^{-1} band but rather show a unique absorption band located at 2711 cm^{-1} (Fig. 9). Therefore, the 2725 cm^{-1} absorption band observed for deuterated samples is not due to talc but to deuterated brucite, $MgOD_2$ (Van der Marel & Beutelspacher, 1976). Indeed, Mg^{2+} resulting from dolomite dissolution in D_2O may react and crystallize as deuterated brucite, which may in turn induce talc particle cementation.

Morphological characterization of talc particles by FTIR

K, the degree of H-D exchange, can be expressed as:

$$K = \frac{S_D}{S_H + S_D}$$

where S_D and S_H represent surface areas of Mg_3OD and Mg_3OH bands at 2711 cm^{-1} and 3676 cm^{-1}, respectively, using a linear baseline. Such measurements were performed only on EDTA-treated

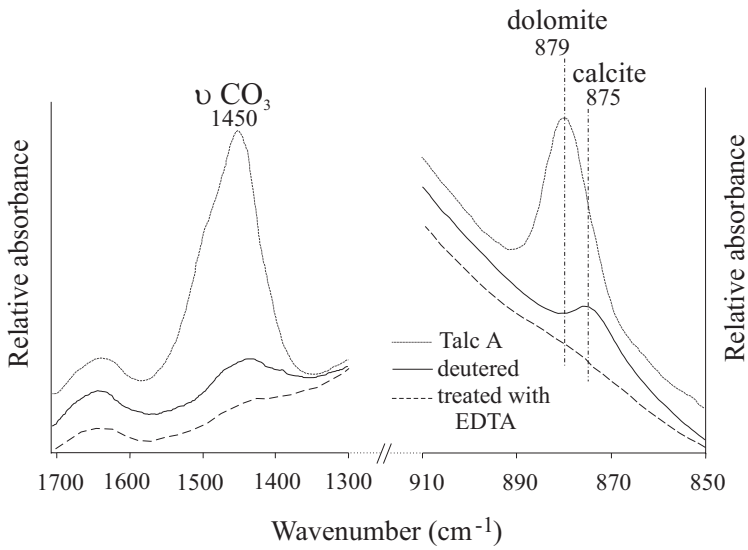

FIG. 7. FTIR spectra of talc A (60 $m^2\ g^{-1}$) before deuteration, after deuteration, and after treatment with EDTA in the 1700–1300 cm^{-1} and 910–850 cm^{-1} regions.

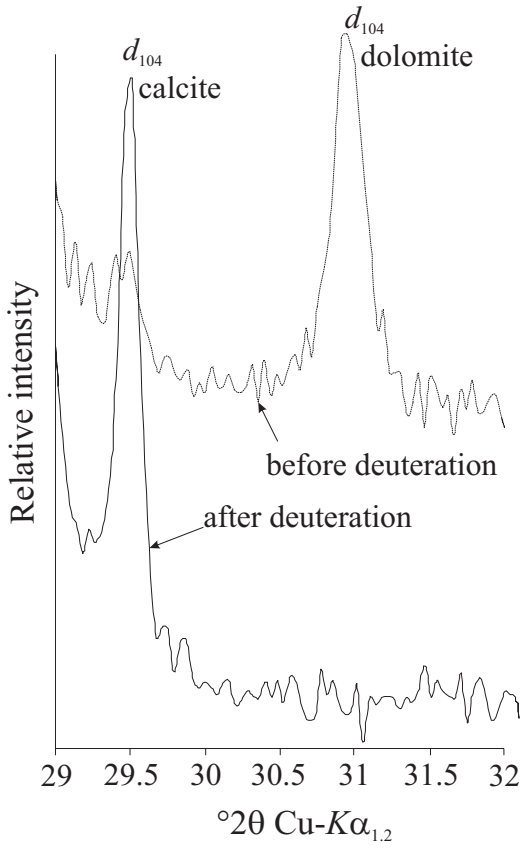

FIG. 8. XRD patterns of talc A (60 $m^2 g^{-1}$) before and after deuteration.

samples to eliminate the influence of the 2725 cm^{-1} band related to deuterated brucite.

A plot of *K vs*. BETSSA reveals a relatively good correlation for the two talc samples (Fig. 10). For both talcs, a polynomial regression describes the increased H-D exchange after milling. Because deuteration is efficient only on the lateral surfaces of talc particles, the progress of H-D substitution is indicative of the relative proportion of basal and lateral surfaces for talc particles having the same specific surface area. For example, for a given specific surface area, H-D substitutions are more abundant for talc A than for talc B (Fig. 10). This indicates that it is possible to differentiate the two talc morphologies, and that in the present case, talc B has a higher basal/lateral surface ratio. This observation is valid whatever the milling (Fig. 10).

CONCLUSIONS

Talc, used as filler in many industrial applications, usually improves the mechanical properties of the resulting composite materials. However, the effect of talc addition on polymers depends heavily on the particle shape and on the crystallinity of the sample; macrocrystalline talc usually leading to better mechanical properties than microcrystalline talc. However, particle morphology (basal surface/lateral surface ratio) is difficult to estimate, especially when two talc samples have similar BETSSA values. The present work shows that it is

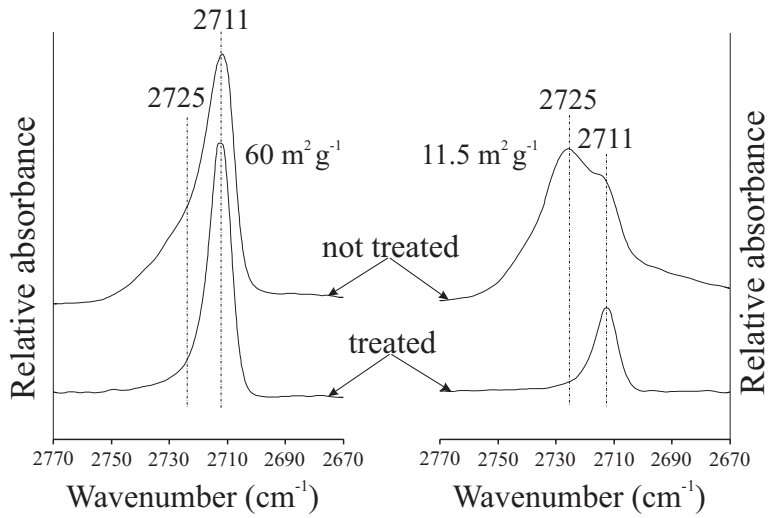

FIG. 9. FTIR spectra after deuteration of talc A (11.5 and 60 $m^2 g^{-1}$) treated with EDTA, and untreated, in the OD region (2770−2670 cm^{-1}).

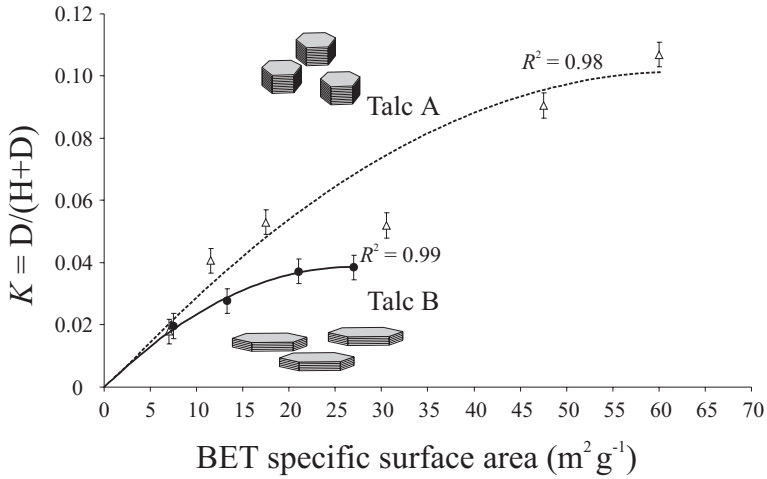

FIG. 10. Correlation between K = D/(H+D) ratio *vs*. BETSSA for talcs A and B. The plot for 30.5 m^2/g for talc A was excluded from the regression. Schematized particle shapes are illustrated to describe the differences in basal/lateral surface ratios of talcs A and B, for the same BET specific surface areas.

possible to overcome this problem using the deuteration technique at 200ºC and saturated water-vapour pressure conditions. Under these experimental conditions, hydrogen atoms located in the hexagonal rings are not exchanged, and the H/D exchange occurs only on lateral surfaces of talc particles.

In addition, the integrated intensity of the νMg_3OD absorption band (2711 cm^{-1}) is proportional to the degree of exchange between H and D. Consistently, experiments carried out using ground talc showed that the intensity of this 2711 cm^{-1} band increases with increasing BETSSA. As a consequence, the correlation between the degree of deuteration K = D/(H+D) and the BETSSA allows an easy characterization of talc morphology even for very fine particles: for the same BETSSA, the talc with lower basal/lateral surfaces ratio shows a higher H-D exchange whatever the milling intensity.

In conclusion, our experiments showed that the deuteration procedure coupled with IR spectroscopy measurements comprises a simple technique for characterization of particle morphology of unknown products. For the same specific surface area, a product with greater lateral surface will lead to increased H-D substitutions. Such morphological characterization is especially relevant in talc polymer applications for which the most lamellar talcs are used. Poorly lamellar talcs reduce the effect of talc filler in polymers giving lower stiffness, hardness and UV protection.

ACKNOWLEDGMENTS

EF is grateful to the S.A. Talc de Luzenac for financial support. Constructive remarks and comments by J. Madejová and an anonymous reviewer, and assistance from Anne Marie Karpoff and Bruno Lanson helped to improved the original manuscript. Technical assistance from University Paul Sabatier (EMPA), Ecole Nationale Supérieure de Chimie (SEM), Hydr'ASA (DRIFT), and Luzenac Europe laboratory (XRF, XRD, BET, FTIR) is acknowledged.

REFERENCES

de Parseval P., Moine B., Fortuné J.P. & Ferret J. (1993) Fluid mineral interactions at the origin of the Trimouns talc and chlorite deposit (Pyrénées, France). Pp. 205–209 in: *Current Research in Geology Applied to Ore Deposits* (P. Fenoll Hach-Ali, J. Torres-Ruiz & F. Gervilla, editors). University of Granada, Spain.

Farmer V.C., Russel J.D. & Ahlrichs J.L. (1968) Characterization of clay minerals by infrared spectroscopy. *Transactions of the 9th International Congress of Soil Science*, **3**, 101–110.

Ferrage E., Martin F., Boudet A., Petit S., Fourty G., Jouffret F., Micoud P., de Parseval P., Salvi S., Bourgerette C., Ferret J., Saint-Gérard Y., Buratto S. & Fortuné J.P. (2002) Talc as nucleating agent of polypropylene: morphology induced by lamellar particles addition and interface mineral-matrix modelization. *Journal of Material Science*, **37**, 1561–1573.

Fortuné J.P., Gavoille B. & Thiebaut J. (1980) Le gisement de talc de Trimouns près de Luzenac (Ariège). *International Geological Congress*, **26**, E10, 43.

Grauby O., Petit S., Enguehard F., Martin F. & Decarreau A. (1991) XRD, EXAFS and FTIR octahedral cation distribution in synthetic Ni-Co kerolites. *Proceedings of 7th Euroclay Conference, Dresden*, **2**, 447–452.

Ishida K. (1990) Identification of infrared OH librational bands of talc-willemseite solid solutions and $Al^{(IV)}$ free amphiboles through deuteration. *Mineralogical Journal*, **15**, 93–104.

Langer K. & Lattard D. (1980) Identification of a low OH valence vibration in zoisite. *American Mineralogist*, **50**, 779–783.

Martin F., Petit S., Grauby O. & Lavie M.P. (1999) Gradual H/D substitution in synthetic germanium bearing talcs: a method for infrared band assignment. *Clay Minerals*, **34**, 365–374.

Menczel J. & Varga J. (1983) Influence of nucleating agents on crystallization of polypropylene. I. Talc as nucleating agent. *Journal of Thermal Analysis*, **28**, 161–174.

Moine B., Fortuné, J.P., Moreau P. & Viguier F. (1989) Comparative mineralogy, geochemistry and conditions of formation of two metasomatic talc and chlorite deposits: Trimouns (Pyrénées, France) and Rabenwald (Eastern Alps, Australia). *Economic Geology*, **84**, 1398–1416.

Russel J.D., Farmer V.C. & Velde B. (1970) Replacement of OH by OD in layer silicates and identification of these groups in infrared spectra. *Mineralogical Magazine*, **37**, 292, 869.

Shirozu H. & Ishida K. (1982) Infrared study of some 7 Å and 14 Å layer silicates by deuteration. *Mineralogical Journal*, **11**, 161–171.

Stubican V. & Roy R. (1961) A new approach to assignment of infrared absorption band in layer-structure silicates. *Zeischrift für Kristallographie*, **115**, 200–214.

Van der Marel H.W. & Beutelspacher H. (1976) *Atlas of Infrared Spectroscopy of Clay Minerals and their Admixtures*. Elsevier Science Publishing Company, Amsterdam.

Wilkins R.W.T. & Ito J. (1967) Infrared spectra of some synthetic talcs. *American Mineralogist*, **52**, 1649–1661.